Length versus radius relationship for ZnO nanowires grown via Vapour Phase Transport

Ruth B. Saunders, Seamus Garry, Daragh Byrne, Martin O. Henry, and Enda McGlynn[*]

School of Physical Sciences, Dublin City University, Dublin, Ireland

E-mail: enda.mcglynn@dcu.ie

Phone: +353 (1)700 5387. Fax: +353 (1)700 5384

Abstract

We model the growth of ZnO nanowires via vapour phase transport and examine the relationship predicted between the nanowire length and radius. The model predicts that the lengths of the nanowires increase with decreasing nanowire radii. This prediction is in very good agreement with experimental data from a variety of nanowire samples, including samples showing a broad range of nanowire radii and samples grown using a lithographic technique to constrain the nanowire radius. The close agreement of the model and the experimental data strongly support supporting the inclusion of a surface diffusion term in the model for the incorporation of species into a growing nanowire.

Introduction

ZnO is a promising semiconducting material with exciting applications and a strong propensity to grow in nanostructured form, displaying a wide range of morphologies[1–3] sensitive to growth

---

[*]To whom correspondence should be addressed

parameters such as temperature, substrate type and the method used to generate source species. Because of this sensitivity and morphological diversity, greater theoretical understanding of the growth is required to reproducibly grow specific ZnO nanostructure morphologies, especially on an industrial scale.

Nanostructure morphology is key to functionality and in particular nanowire dimensions are relevant to many practical applications of ZnO nanowires, such as lasing threshold,[4] gas sensing applications[5] and voltage-current characteristics.[6] The relationship between the length and radius of a nanowire also gives us information about the growth mechanism of the nanowire. For all these reasons a clear understanding of the relationship between nanowire length and radius, and the underlying growth mechanism, are important goals for future applications of such materials.

The growth rate and final length of crystal whiskers has been the subject of many studies on various materials. Various hypotheses for the growth mechanisms in Vapour Solid (VS) growth have been proposed, including that only atoms striking the top of the whisker contributes to growth,[7] and that atoms striking the whisker elsewhere and diffusing to the top also contribute.[8–11] The latter hypothesis has emerged as correct based on detailed studies.[11] Further complications are found for the case of vapour-liquid-solid (VLS) growth, where the catalyst particle properties strongly affect growth behaviour.[12–14] For the specific case of ZnO nanowire growth via a VS growth mechanism, very little work has been reported. Kim et al.[15] studied ZnO nanowires grown via Vapour Phase Transport (VPT) on small Au clusters. Oh et al.[16] studied ZnO and In-doped ZnO nanowires grown via VPT on both AuGe and Ti deposited Si substrates while Hejazi and Hosseini also studied Au catalysed ZnO growth.[17] In all these cases the influence of the metal/alloy catalyst is likely to complicate the situation and consequently the growth in the common VS mode remains essentially unexplored.

This paper presents a model specifically derived for the growth rate of ZnO nanowires via a VS growth mechanism using the common VPT growth method (and Carbothermal Reduction (CTR) of ZnO by graphite). Our previous work concentrated on generation and transport of source species and condensation/nucleation on the substrate.[18,19] This paper builds on that work and specifically

examines the kinetics of VPT growth of ZnO nanowires. We describe a model to calculate the growth rate of ZnO nanowires, allowing us to study the relationship between the length and radius of a ZnO nanowire. We also apply this model (with a reduced number of free parameters (using previous results from our group) to experimental results by calculating the number of atoms arriving at the nanowire. The model predicts the nanowire lengths increase with decreasing nanowire radii, in very good agreement with our experimental data from a variety of nanowire samples, including samples showing a broad range of nanowire radii and samples grown using a lithographic technique to constrain the nanowire radius. The close agreement of the model and the experimental data strongly support the inclusion of a surface diffusion term in the model for the incorporation of species into a growing nanowire. Given the paucity of previous theoretical work on this important aspect of ZnO nanostructures, we believe that the present work makes a significant addition to the literature, particularly since it builds on our previous work and makes use of the quantitative results therein to reduce the number of free parameters in our present model.

Experimental

Growth substrates were prepared with a ZnO buffer layer using a method combining drop coating and chemical bath deposition (CBD)[20] to provide energetically suitable nucleation/accommodation sites for ZnO nanowire growth. Non-metallic ZnO seeds and buffer layers were used, to eliminate the possibility of a vapour-liquid-solid (VLS) growth mode and ensure a vapour-solid (VS) growth mode. Equal amounts (usually 0.06 g) of ZnO powder and graphite are mixed together in a pestle and mortar. The resulting mixture is placed in an alumina boat and spread evenly over a width of 1.5 cm. Two rectangles of silicon are placed on top of the alumina boat. The prepared substrate (a buffer layer of ZnO on a Si/SiO$_2$ substrate) is placed face down on the silicon supports directly above the powder. The sample is ~ 1 cm above the powders. This boat is then placed in the centre of a quartz tube, positioned in a Lenton Thermal Designs single temperature zone horizontal tube furnace as illustrate in Figure 1. One end of the furnace is attached to gas lines for argon (and in

some cases oxygen) via Mass Flow Controllers (Analyt GFC17). The other end is connected to an exhaust line. The pressure in the furnace is 1 atm, as the furnace is open to the external atmosphere, via the exhaust. An argon flow of 90 sccm is used to flush the furnace for 10-15 minutes prior to growth. This flow of argon is continued for the duration of the growth. The furnace is heated to 1200 K, which takes approximately 10 minutes and is kept at this temperature for one hour. The furnace is then allowed to cool for several hours before the argon is turned off and the sample removed.
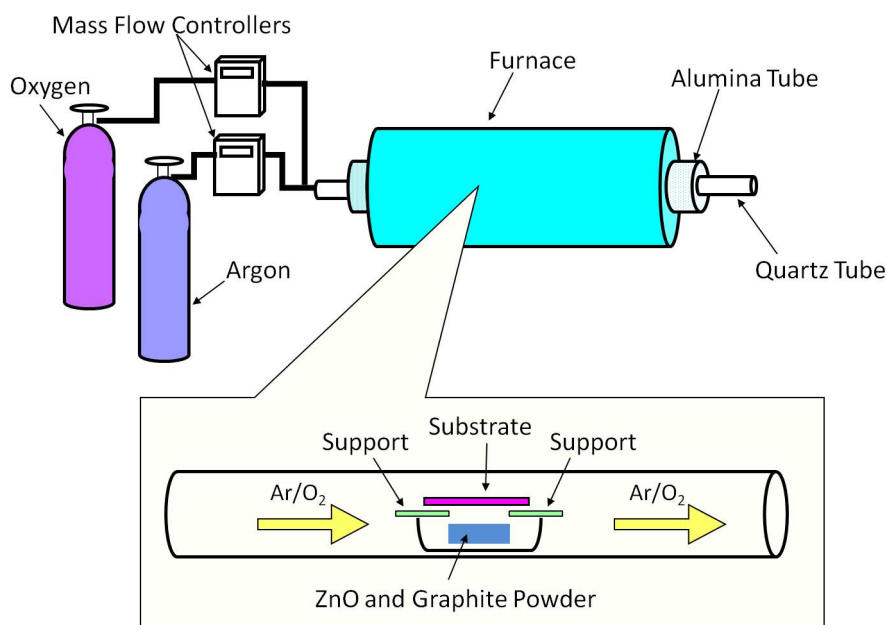
Figure 1: Illustration of experimental set up for VPT growth

In addition to the growth method described above, VPT growths in a specific amount of O_2 were also performed. To remove the residual O_2, the furnace is flushed for 50 minutes with Ar before increasing the temperature. When a VPT growth is attempted after this purge is performed no ZnO nanowire growth is observed, indicating that all of the residual O_2 has successfully been removed. After this 50 minute flushing period, 2 sccm of O_2 is introduced to the gas flow mix. This allows a better estimate of the precise gaseous composition arriving at the nanowire.

In addition to growth on unpatterned ZnO buffered substrates, arrays of ZnO nanowires are also grown by performing a VPT growth on a patterned ordered silica template produced by nanosphere

4

lithography.[21] A substrate prepared with a ZnO buffer layer is coated with a self-assembled mono-layer of 1.5 μm diameter polystyrene nanospheres, using the water transfer method, and allowed to dry. The resulting sample was annealed at 110 ° C for 40 s. An acid catalyzed silica sol, of 0.5 ml tetraethyl orthosilicate and 0.5 ml hydrochloric acid in 20 ml of ethanol, was deposited into the interstitial spaces left exposed by the close packed nanosphere pattern. The latter was then removed by ultra-sonication in toluene first, followed by acetone. The remaining hexagonal silica surface lattice was densified by annealing at 400 ° C with a 10 ° C/min ramp rate. An SEM image of the patterned template is shown in Figure 2. The majority of the substrate is covered by silica and ZnO will not nucleate/deposit in those areas. Only at the centre of the silica depressions, where the nanospheres were located, is the underlying ZnO buffer layer exposed, and thus only there will ZnO nanowire growth proceed during VPT growth. The radius of the exposed buffer layer regions on the patterned substrate tends to be rather uniform and leads to a uniformity in radius of the nanowires grown by VPT subsequently. This was finally used as the substrate on which to deposit the ZnO nanowire arrays by VPT.
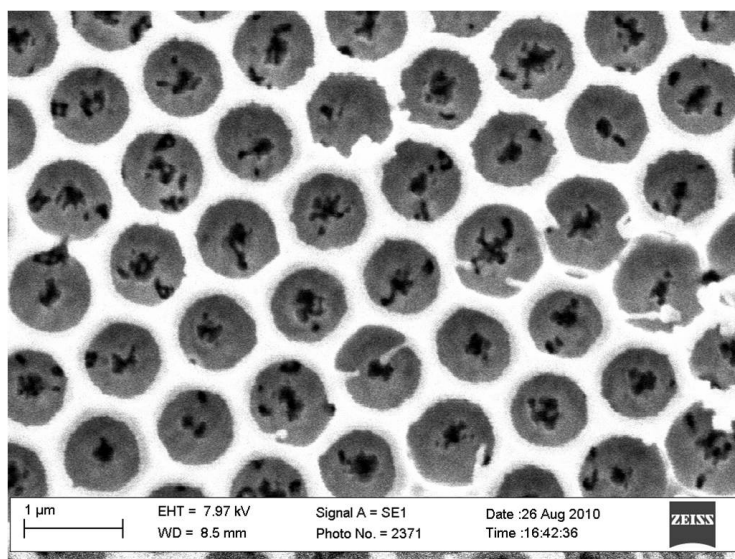

Figure 2: SEM image of the silica template produced by nanosphere lithography

The ZnO nanowires were then examined using a scanning electron microscope (SEM, Karl-Zeiss EVO series). The images from the SEM are analyzed using ImageJ software.[22]

Model for growth rate

The model to find the growth rate of ZnO nanowires follows the model for mass transport model derived for metal-particle assisted growth of III/IV nanowires developed by J. Johansson[14](including the assumptions on which that model is based as relevant here, *i.e.* steady-state diffusion on the substrate and nanowire walls towards the nanowire top and that the interwire separation is sufficiently large to prevent shadowing effects/competition for available source material). Slight amendments to the existing model were made to take account of the slightly different morphology observed in our grown nanowires, with flat top surfaces, compared to those with rounded top surfaces considered in the original model. Specifically, the model is altered for application to VS growth of ZnO nanowires on a ZnO buffer layer by considering a circular collection area for atoms/molecules on the top of the nanowire as opposed to a hemispherical collection area.

Growth is assumed in this model to only take place only at the top of the nanowire (*i.e.* material is incorporated only at the top surface of the nanowire), the radius is assumed to be constant throughout the growth. ZnO is an anisotropic material, with different values of surface energy for different faces which leads to preferential growth along the *c*-axis. The top of the nanowire, the (0001) basal plane surface, is a polar face that is either Zn or O terminated whereas the side faces of the nanowire are non polar. Although atom/molecule incorporation on the sides of the nanowire is possible, here we consider the ideal case where incorporation only takes place on the top of the nanowire. This assumption is supported by the extensive body of experimental evidence in the literature reporting ZnO nanorod/nanowire growth with the long axis parallel to the crystallographic c-axis and with large aspect ratios, in addition to the c-axis texture of most ZnO thin films.[23] Atoms/molecules can arrive from the vapour to the top of a growing nanowire in three ways as illustrated in Figure 3.

1: Atoms/molecules arrive directly on the top of the growing nanowire.
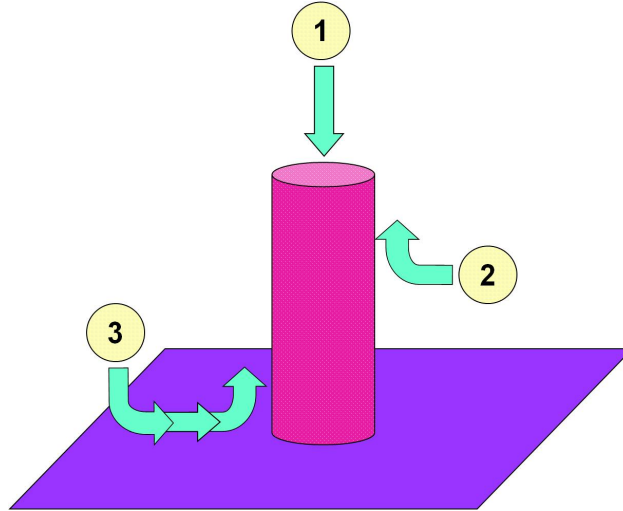2: Atoms/molecules impinge on the sidewalls of the growing nanowire and
   diffuse to the top.

Figure 3: Illustration of the impingement of molecules on a growing nanowire

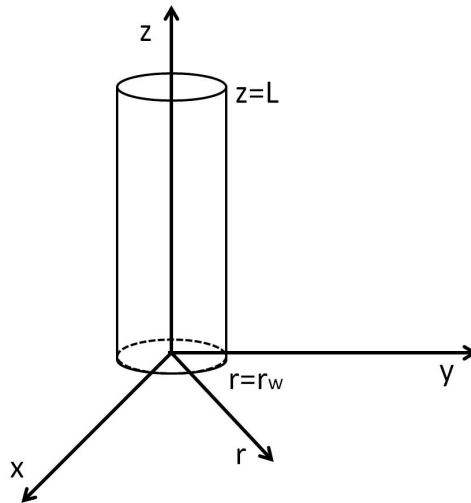3: Atoms/molecules impinge onto the substrate, diffuse to the nanowire and then up the sidewall to the top.

Figure 4: Schematic of growing nanowire

The number density of atoms/molecules on the substrate is described by:[14]

$$D_s \nabla^2 n_s - \frac{n_s}{\tau_s} + J_s = \frac{\partial n_s}{\partial t} \qquad (1)$$

Where J_s is the impingement rate of molecules onto the substrate, τ_s is the mean lifetime of the molecule on the substrate, n_s is the density of molecules on the substrate and D_s is the diffusion constant for molecules on the substrate. The diffusion length of molecules on the substrate λ_s is given by: $\lambda_s = \sqrt{D_s \tau_s}$. Solving this with the boundary condition, $n_s(r = r_w) = 0$ (see Figure 4 for a schematic diagram explaining the coordinates used), gives the number density of atoms/molecules on the substrate surface, which contains modified Bessel functions of the second kind, K_0:

$$n_s(r) = J_s \tau_s \left[1 - \frac{K_0(\frac{r}{\lambda_s})}{K_0(\frac{r_w}{\lambda_s})} \right] \qquad (2)$$

The number density of atoms/molecules on the nanowire sidewall can be described by the one-dimensional diffusion equation where now the subscript w denotes values on the sidewall of the nanowire, with the main symbols retaining the same meaning (D for diffusion coefficient etc.):[14]

$$D_w \frac{\partial^2 n_w}{\partial z^2} + J_w - \frac{n_w}{\tau_w} = \frac{\partial n_w}{\partial t} \qquad (3)$$

This equation with the boundary conditions, $n_w(z = L) = 0$ and $D_w \frac{\partial n_w}{\partial z}\big|_{z=0} = -D_s \frac{\partial n_s}{\partial r}\big|_{r=r_w} = J_{sw}$ gives the density of molecules on the sidewall of the nanowire:

$$n_w = J_w \tau_w \left[1 - \frac{\text{Cosh}(\frac{z}{\lambda_w})}{\text{Cosh}(\frac{L}{\lambda_w})} \right] - \frac{J_{sw} \lambda_w}{D_w} \frac{\text{Sinh}(\frac{L-z}{\lambda_w})}{\text{Cosh}(\frac{L}{\lambda_w})} \qquad (4)$$

The flux from the substrate to the nanowire is given by J_{sw}, whose exact form is:

$$J_{sw} = D_w \frac{\partial n_w}{\partial z}\bigg|_{z=0} = -J_s \lambda_s \frac{K_1(\frac{r_w}{\lambda_s})}{K_0(\frac{r_w}{\lambda_s})} \qquad (5)$$

The contribution of molecules from the sidewalls and the substrate to the length rate is:

$$\frac{\partial L}{\partial t} = -D_w \frac{\partial n_w}{\partial z}\bigg|_{z=L} \times 2 \frac{\Omega}{r_w} \qquad (6)$$

Combining this with the contribution to the growth rate from direct impingement to the top of the

nanowire ΩJ_t (where Ω is the molecular volume of ZnO), and assuming that all the impingement rates are equal (*i.e.* $J_s = J_w = J_t = J$, as implied by the assumption of no shadowing/competition effects), gives the total growth rate of ZnO nanowires:

$$\frac{\partial L}{\partial t} = \Omega J + \frac{2\Omega J \lambda_w}{r_w} \text{Tanh}\left(\frac{L}{\lambda_w}\right) - \frac{2\Omega J_{sw}}{r_w \text{Cosh}(\frac{L}{\lambda_w})} \tag{7}$$

We integrated the growth rate from zero to the growth time to give the length of the nanowire. These calculations were performed using MATLAB.[24] The model shows that when molecules impinging directly onto the nanowire top are considered alone (i.e the growth rate $= \Omega J$), the predicted length of the nanowire is identical regardless of the nanowire radius. When molecules diffusing from the side walls are included in the model, the calculated length of the nanowire decreases with increasing radius.

There are no reported values for the diffusion length of Zn atoms on the sidewalls of ZnO nanowires or on the ZnO buffer layer-covered substrate. We thus estimate these parameters to best fit the data, as $\lambda_s = \lambda_w = 100$nm. However we note, in support of these estimates, that the values of the estimates we use are of a comparable order of magnitude to other values reported for Zn and similar materials. In their study of ZnO nanowires, Oh *et al.*[16] find a best fit using a diffusion length of 180 nm for Zn adatoms on ZnO nanowire sidewalls. Johnasson *et al.* find a diffusion length for Ga on GaP nanowire sidewalls of ~ 350 nm gives the best fit between experimental results and theory. In a study of the diameter dependent growth rate of InAs nanowires, Froberg *et al.*[25] find a value of 130 nm for the diffusion length of In atoms on InAs gives the best results for comparison to experimental results.

Figure 5 shows the length of the nanowires, as a function of radius for a growth duration of 30 minutes, exploring the contribution of each of the terms on the RHS of equation 7. The net effective impingement rate is estimated from the number of molecules necessary to have the observed density of ~ 40 nanowires/μm^2 of length 2 μm and radius 37.5 nm over the growth time to be $J = 0.85 \times 10^{19}$mc/m^{2}s. The length of the nanowire calculated using a model that includes

only molecules impinging on the top of the nanowire (term 1 of equation (7) above) is shown. These lengths are constant for all nanowire radii. Figure 5 also shows the length when molecules diffusing from the sidewall (terms $1 + 2$) and molecules from the sidewall and substrate (terms $1 + 2 + 3$) are included in the model. There is no difference between these curves, indicating that the contribution of term 3 to the growth is negligible after the nanowire length exceeds the Zn diffusion length scale. After a growth duration of 30 minutes the molecules from the substrate no longer reach the top of the nanowire, so including this term does not affect the final length. The lengths shown in Figure 5 decrease with increasing radius.
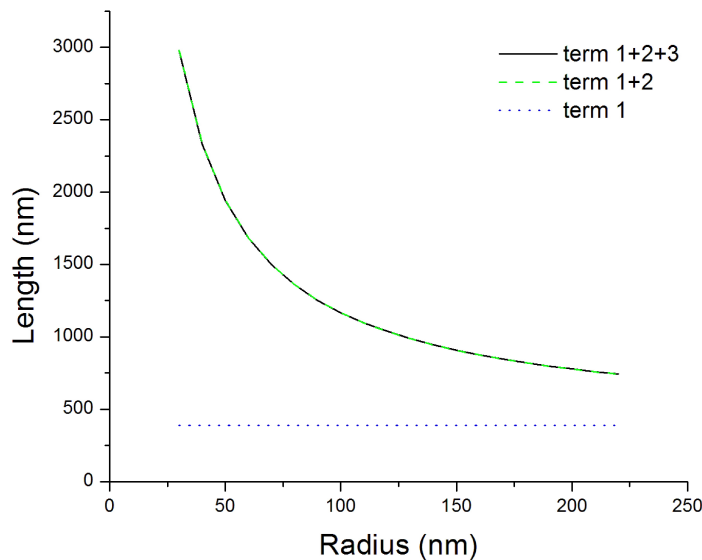
Figure 5: Nanowire length as a function of radius for a growth duration of 30 minutes to compare relative contribution of terms in model

Results

Here we detail the comparison of the lengths calculated by the above model to experimental results. There are three possible general outcomes of these measurements:

1. All of the nanowires are the same length regardless of nanowire radius. This would suggest that

only molecules directly impinging on the top of the nanowire contribute to nanowire growth.

2. The length of the nanowires increases with decreasing radius, *i.e.* thinner nanowires are longer than thicker ones. This supports the need for inclusion of terms to account for molecules diffusing from the sidewalls of the nanowires to the top.

3. The length of the nanowires increases with increasing radius. This would indicate another physical effect, not considered in our analysis, at work during the growth.

ZnO nanowires grown via VPT

Figure 6 shows the results of VPT growth at a temperature of 1200 K for a duration of 1 hour. This figure shows clearly that ZnO nanowires with different radii have different lengths. The radii are thought to be determined by the underlying ZnO buffer layers, specifically the dimensions of the ZnO crystallites deposited by CBD. The measurements of these nanowire lengths and radii are shown in Figure 7(a) and Figure 7(b). The length as a function of radius found using the model is also shown. There is a significant degree of scatter in these measurements, due primarily to the random effects of shadowing of growing nanowires by other nanowires in close proximity (discussed below), as well as the possibility of some variations in the local impingement rate of source material from the vapour phase due to local turbulence and other effects. Hence we have performed averages of the experimental data, but there is no natural choice of dependent and independent variable between the nanowire length and and radius, so we have analysed the data treating first the radius and then the length as the independent variable. In Figure 7(a) the large open circles and associated error bars represent averages over the experimental nanowire length data shown by smaller black dots, binned according to nanowire radius, with a bin size chosen to ensure a reasonable (greater than five) number of data points in each bin, generally in the region of 20-30 nm. In Figure 7(b) the large open circles and associated error bars again represent averages, now over nanowire radii, binned according to nanowire length, with a variable bin size generally in the region of 300-400 nm. This VPT growth method makes use of the residual O_2 present in the furnace after a brief flushing period, the exact number of atoms/molecules arriving at the sample

11

substrate is unknown. We are unable to calculate an exact impingement rate for Zn atoms or O_2 molecules as we do not have a value for the partial pressure of the O_2 present in the furnace. We use an estimated net effective impingement rate of $J = 0.85 \times 10^{19} mc/m^2 s$. While the growth time is 1 hour, we performed a series of timed experiments which determined that the actual effective duration of nanowire growth is 30 minutes, with the residual oxygen being depleted and no further growth seen after 30 minutes.
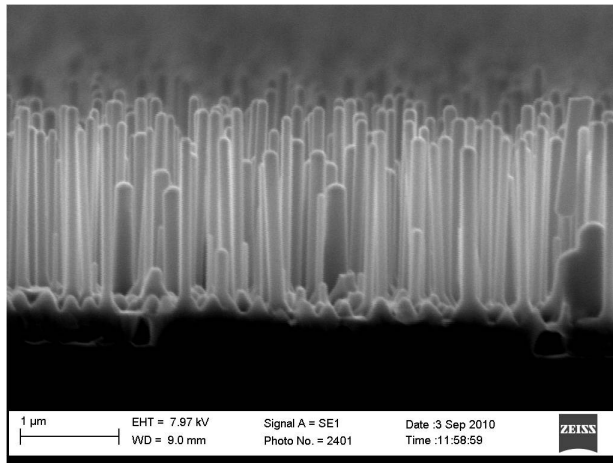
(a)
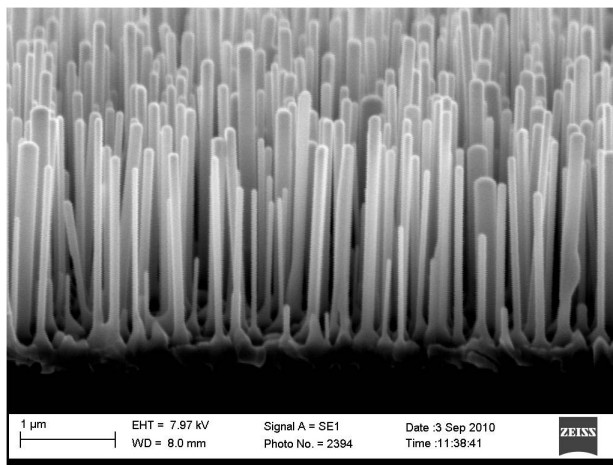
(b)

Figure 6: SEM images of ZnO nanowires grown via VPT grown at 1200 K for 1 hour, (a) cross-sectional view, (b) tilted at 75° view
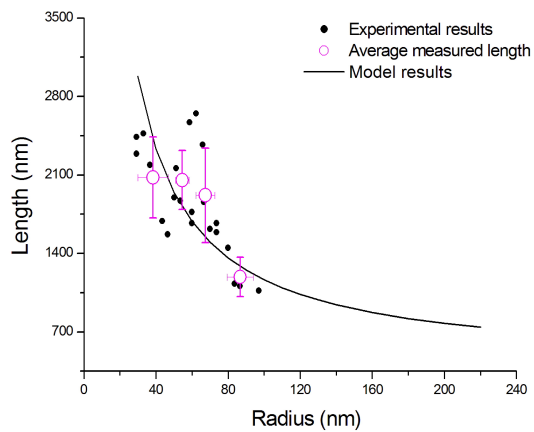
(a)
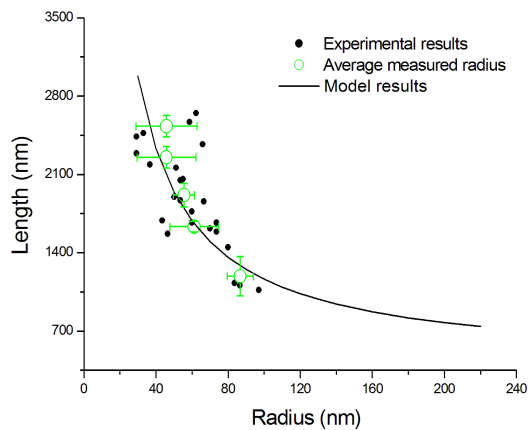
(b)

Figure 7: Nanowire length as a function of radius for sample with a growth time of 30 minutes and statistical analysis of data, as described in text

ZnO nanowires grown via VPT in a specific amount of O_2

The nanowires discussed in this section were grown in a specific amount of O_2 at a temperature 1200 K. This allows the calculation of a more precise value for the number of molecules arriving at the substrate. The impingement rate of molecules from a vapour can be calculated from the partial pressure of that vapour using the Knudsen relation:[26]

$$J = \frac{p}{\sqrt{2\pi m k_b T}} \qquad (8)$$

We have found previously[19] that the number of Zn molecules arriving at the substrate ($J_{Zn} = 2.79897 \times 10^{26} \mathrm{mc/m^2s}$) exceeds the number of O_2 molecules ($\alpha_{O_2} J_{O_2} = 3.95741 \times 10^{19} \mathrm{mc/m^2s}$) present. However, we take the number of O_2 molecules as the number of arriving molecules because the number of Zn molecules that will become solid ZnO is limited by the amount of O_2 available. Using the partial pressure of O_2, we calculate the impingement rate. The partial pressure for O_2 is calculated from the relative value in the gas flow mix. The sticking coefficient for oxygen is not unity, as it is a diatomic molecule, and the dissociation of oxygen molecules to react with Zn atoms is a complex process. We find the sticking coefficient α_{O_2} using an empirical expression given by Rojo *et al.*[27]

$$\alpha_{O_2} = (0.27966) \exp\left[\frac{-14,107.9578}{T}\right] \qquad (9)$$

Figure 8(a) shows the measurements of the lengths and radii of ZnO nanowires grown for a duration of 40 minutes and with a similar statistical analysis to that shown for the data in Figure 7, treating the radius as the independent variable in Figure 8(a) and the length as the independent variable in Figure 8(b). In both Figure 8(a) and Figure 8(b) the large open circles and associated error bars represent averages over the experimental data shown by smaller black dots. This figure also shows the calculated lengths for a growth duration of 40 minutes and for an impingement rate of $J=\alpha J_{O_2}$ and $J=0.75\alpha J_{O_2}$. The measurements show again an overall decrease in nanowire length

with an increase in nanowire radius. The values for lengths found for $J=0.75\alpha J_{O_2}$ are in good agreement with the measured values.
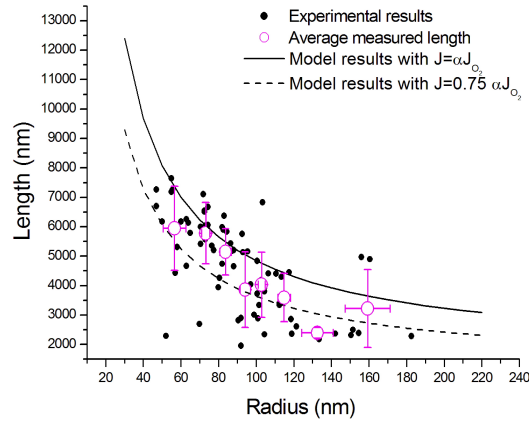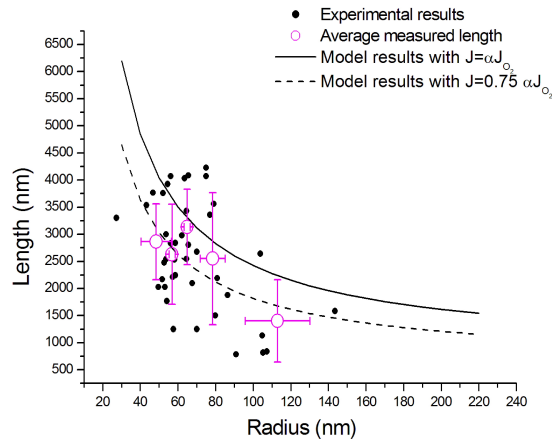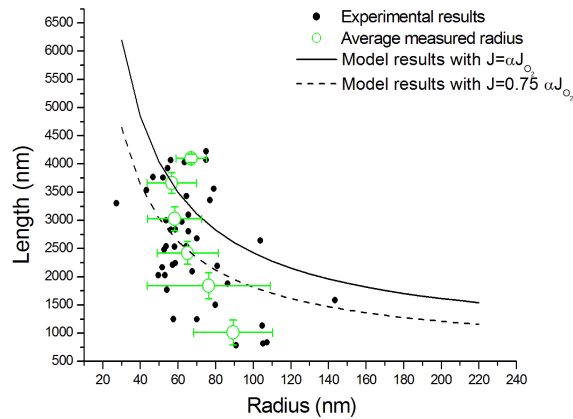

(a)
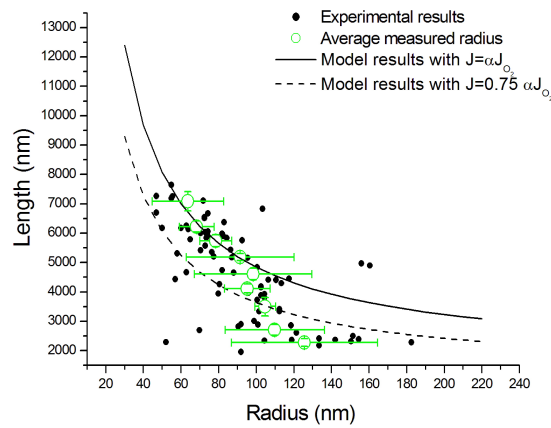
(b)

Figure 8: Nanowire length as a function of radius for sample grown for 40 minutes with a specific amount of O_2 and statistical analysis of data, as described in text

Figure 9 shows the results for nanowires that were grown for 20 minutes in a specific amount of O_2 and with a similar statistical analysis to that shown for the data in Figure 7 and Figure 8, treating the radius as the independent variable in Figure 9(a) and the length as the independent variable in Figure 9(b). In both the large open circles and associated error bars represent averages over the experimental data shown by smaller black dots. These nanowires are, as expected, shorter

overall than those grown for a duration of 40 minutes. The calculated lengths for a duration of 20 minutes are compared to the measured values in Figure 9. Again the measured values show better agreement with the model using a molecule impingement rate $J=0.75\alpha J_{O_2}$.

(a)

(b)

Figure 9: Nanowire length as a function of radius for sample grown for 20 minutes with a specific amount of O_2 and statistical analysis of data, as described in text

ZnO nanowires grown via VPT on an ordered arrays

There are issues to be addressed in the application of this model to our growth system. In the derivation of the model, it is assumed that the interwire spacing of the nanowires is large, which

allows us to claim that the impingement of atoms /molecules onto the top of the wire is equal to the impingement of atoms/molecules on the sidewalls. As can be seen in Figure 6, the nanowire density on most samples is large, indicating that the impingement rate of molecules on the sidewalls is less than the impingement rate of molecules onto the top of the nanowire due to shadowing effects and this is likely to be a cause of a substantial amount of the scatter of the experimental data seen in Figure 7, Figure 8 and Figure 9, as mentioned previously. One way to address this is to reduce the nanowire density by performing VPT growth on an ordered array template.

Figure 10 shows the results of a VPT growth on a pattern ordered template array with a spacing of 1.5 μm. Nanowires grown on these templates are forced to have a narrower range of radii determined by the available contact area to the underlying ZnO buffer layer, as mentioned previously. We would expect to find that nanowires with identical radii will have identical lengths.
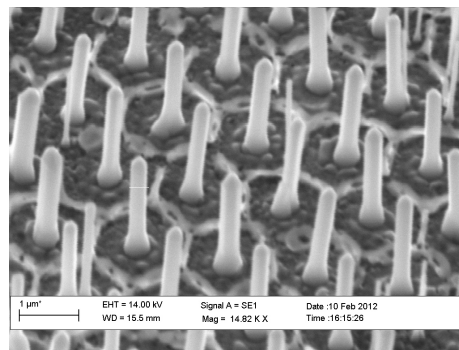

Figure 10: SEM image of nanowire array with spacing of 1.5 μm

The lengths of ZnO nanowires grown on a template with spacing of 1.5 μm as a function of radius are shown in Figure 11 and with a similar statistical analysis to that shown previously, though for the data shown in Figure 11 the scatter in the data is sufficiently small to allow a single binning of both radius and length. The large open circles represent averages over the experimental data shown by smaller black dots (the error bar for the average length is smaller than the symbol, while the error bar for the radius is shown). For comparison the data for a non spaced array are also shown as small open black circles (same data as shown in Figure 7, which was from a sample grown in identical conditions except for the absence of substrate templating, *i.e.* at a temperature

17

of 1200 K for a duration of one hour). The experimental results show that a much smaller range of lengths and radii for ZnO nanowires grown on an ordered template. The experimental results show good agreement with the values predicted by the model and also confirm that shadowing effects/competition for available source material are an important contribution to the scatter observed for the experimental data in Figure 7, Figure 8 and Figure 9, as mentioned previously.
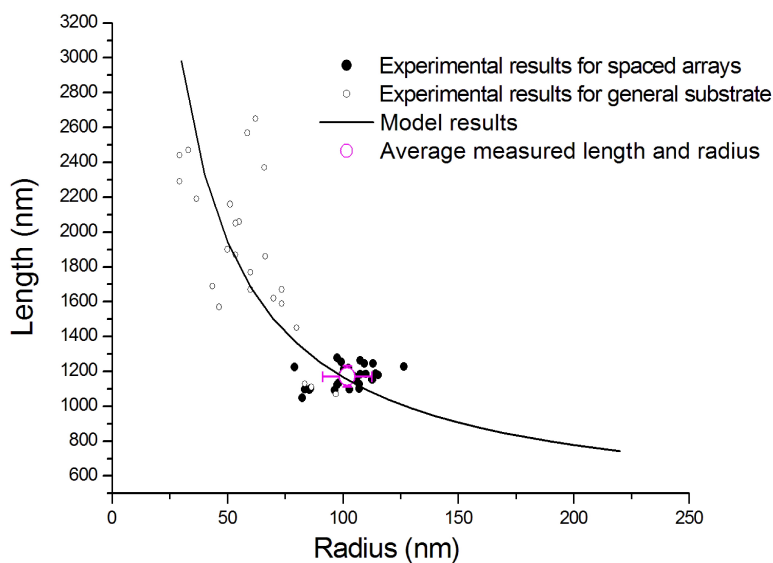

Figure 11: Nanowire length as a function of radius for nanowire array with spacing of 1.5 μm for a growth time of 30 minutes and statistical analysis of data, as described in text

Conclusions

This paper describes a model to calculate the growth rate of ZnO nanowires. The model includes contributions of molecules from direct impingement onto the top of the nanowire and molecules diffusing from the sidewalls and from the substrate.

Measured values of the length and radius of nanowires grown via VPT on ZnO buffer layers show that thinner nanowires are longer than thicker nanowires, supporting the inclusion of molecules diffusing from the sidewalls in the model. For growths using the residual O_2 in the

furnace, it is impossible to accurately compare the predicted nanowire dimensions with the actual measured values, as both the impingement rate of molecules and the diffusion lengths of the molecules are unknown. However, using an effective impingement rate deduced from the final nanowire density and dimensions, good agreement with experimental results is found. When growths are performed in a specific amount of O_2, the impingement rate can be calculated. The best agreement is found for an impingement rate that is 75% the exact calculated value. This is a reasonable estimate for the number of molecules arriving at the nanowires and is consistent with the fact that the calculated pressure and impingement rates are upper bounds based on thermodynamics.[19] The lengths calculated for two different growth times agree with the measured values, subject to the caveat above, showing good agreement for the predicted variation of nanowire lengths with time with the average measured lengths showing an increase in value with decreasing radius.

Overall the experimental results support the inclusion of molecules diffusing from the sidewalls in a model to calculate the growth rate and radius dependency of the length of ZnO nanowires grown via VPT. We believe this work is novel in terms of applying a diffusion based model to the growth of ZnO nanowires because it uses an approach specifically derived for the growth of ZnO nanowires via a VS mechanism and by the use of a largely parameter-free analysis to deduce the impingement rate of atoms on the nanowire. This work may also provide a platform from which to begin comparisons between different ZnO nanostructure growth methods such as VPT and CBD, since studies of morphology variation with growth conditions in the latter CBD method have already been reported,[3] with some interesting similarities apparent between the two methods.

Acknowledgements

References

[1] Grabowska, J.; Meaney, A.; Nanda, K.; Mosnier, J.; Henry, M.; Duclere, J.; McGlynn, E. *PHYSICAL REVIEW B* **2005**, *71*.

[2] Wang, Z. *JOURNAL OF PHYSICS-CONDENSED MATTER* **2004**, *16*, R829–R858.

[3] Zainelabdin, A.; Zaman, S.; Amin, G.; Nur, O.; Willander, M. *CRYSTAL GROWTH & DESIGN* **2010**, *10*, 3250–3256.

[4] Gruzintsev, A. N.; Emelchenko, G. A.; Red'kin, A. N.; Volkov, W. T.; Yakimov, E. E.; Visimberga, G. *SEMICONDUCTORS* **2010**, *44*, 1217–1221.

[5] Spencer, M. J. S. *PROGRESS IN MATERIALS SCIENCE* **2012**, *57*, 437–486.

[6] Yang, Z.; Wen, B.; Melnik, R.; Yao, S.; Li, T. *APPLIED PHYSICS LETTERS* **2009**, *95*.

[7] Sears, G. *ACTA METALLURGICA* **1955**, *3*, 361–366.

[8] Gomer, R. *JOURNAL OF CHEMICAL PHYSICS* **1958**, *28*, 457–464.

[9] Ruth, V.; Hirth, J. *JOURNAL OF CHEMICAL PHYSICS* **1964**, *41*, 3139–&.

[10] Blakely, J.; Jackson, K. *JOURNAL OF CHEMICAL PHYSICS* **1962**, *37*, 428–&.

[11] Parker, R.; Anderson, R.; Hardy, S. *APPLIED PHYSICS LETTERS* **1963**, *3*, 93–95.

[12] Givargizov, E. *JOURNAL OF CRYSTAL GROWTH* **1975**, *31*, 20–30.

[13] Schubert, L.; Werner, P.; Zakharov, N.; Gerth, G.; Kolb, F.; Long, L.; Gosele, U.; Tan, T. *APPLIED PHYSICS LETTERS* **2004**, *84*, 4968–4970.

[14] Johansson, J.; Svensson, C.; Martensson, T.; Samuelson, L.; Seifert, W. *JOURNAL OF PHYSICAL CHEMISTRY B* **2005**, *109*, 13567–13571.

[15] Kim, D. S.; Goesele, U.; Zacharias, M. *JOURNAL OF CRYSTAL GROWTH* **2009**, *311*, 3216–3219.

[16] Oh, S.; Jung, M.; Koo, J.; Cho, Y.; Choi, S.; Yi, S.; Kil, G.; Chang, J. *PHYSICA E-LOW-DIMENSIONAL SYSTEMS & NANOSTRUCTURES* **2010**, *42*, 2285–2288.

[17] Hejazi, S. R.; Hosseini, H. R. M. *JOURNAL OF CRYSTAL GROWTH* **2007**, *309*, 70–75.

[18] Saunders, R. B.; McGlynn, E.; Biswas, M.; Henry, M. O. *THIN SOLID FILMS* **2010**, *518*, 4578–4581.

[19] Saunders, R. B.; McGlynn, E.; Henry, M. O. *CRYSTAL GROWTH & DESIGN* **2011**, *11*, 4581–4587.

[20] Byrne, D.; McGlynn, E.; Kumar, K.; Biswas, M.; Henry, M. O.; Hughes, G. *CRYSTAL GROWTH & DESIGN* **2010**, *10*, 2400–2408.

[21] McCarthy, E.; Garry, S.; Byrne, D.; McGlynn, E.; Mosnier, J. P. *JOURNAL OF APPLIED PHYSICS* **2011**, *110*.

[22] http://rsbweb.nih.gov/ij/.

[23] E. McGlynn, J.-P. M., M.O. Henry In *"ZnO wide bandgap semiconductor nanostructures: growth, characterisation and applications" Chapter 14 (pages 575-624) of volume II of the Handbook of Nanoscience and Technology*; Narlikar, A., Y.Y.Fu,, Eds.; Oxford University Press, UK, 2009.

[24] MATLAB: mathworks website: http://www.mathworks.co.uk/products/matlab/.

[25] Froberg, L. E.; Seifert, W.; Johansson, J. *PHYSICAL REVIEW B* **2007**, *76*.

[26] Smith, D. L. *Thin-Film Deposition, Principles and Practice*; McGraw-Hill, 1995.

[27] Rojo, J. C.; Liang, S.; Chen, H.; Dudley, M. *Proceedings of Society of Photo-Optical Instru-mentation Engineers (SPIE) Conference Series* **2006**, *6122*, 97–104.

For Table of contents use only

Length versus radius relationship for ZnO nanowires grown via Vapour Phase Transport

Ruth B. Saunders, Seamus Garry, Daragh Byrne Enda McGlynn, Martin O. Henry

This paper describes a model of the growth of ZnO nanowires via vapour phase transport and examines the relationship between the nanowire length and radius. The model predicts that nanowire lengths increase as their radii decrease, which strongly agrees with experimental measurements of ZnO nanowires grown via vapour phase transport.
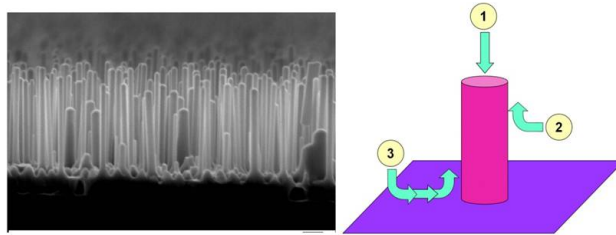

Figure 12: Table of contents graphic